



# A compact displacement sensor for non-intrusive concentration measurements of flowing liquid



Ruey-Ching Twu\*, Jheng-Yu Chen

Department of Electro-Optical Engineering, Southern Taiwan University of Science and Technology, No. 1 Nan-Tai Street, Yung Kang, Tainan 71005, Taiwan

## ARTICLE INFO

### Article history:

Received 5 August 2017

Received in revised form 15 October 2017

Accepted 23 October 2017

### Keywords:

Displacement sensor

Homodyne interferometer

Non-intrusive measurement

Chemical concentration

## ABSTRACT

A compact displacement sensor (CDS) was proposed to be applied as a non-intrusive concentration measurement of flowing liquid by employing a phase-interrogation in a homodyne interferometer. To verify the feasibility of the proposed CDS, a measurement setup was constructed and a series of experiments were performed. The experimental results show that a good linear property between the phase change and the concentration variation are achievable. The disposable and cheap acrylic container potentially provides simple and repeatable concentration measurements. The best measurement resolutions of the weight percentage are 0.015% and 0.013% for the flowing salt and hydrochloric acid solutions, respectively. According to the experimental results, the non-intrusive technique is also useful for real-time quality monitoring of a flowing liquid on a production line.

© 2017 Elsevier B.V. All rights reserved.

## 1. Introduction

The concentration of liquid is an important parameter for quality control in food, chemicals, and pharmaceutical manufacturing [1–5], since the refractive index (RI) and resistivity of the liquids are dependent on the concentrations as well as the weight ratios of the mixture. Typically, sensing heads utilizing electrical and optical characterizations have been developed to analyze concentration variations [3–5]. Especially, liquids mixed with different contents or chemical reactions in manufacturing can be easily monitored through sensing heads. The schemes of conductivity measurements are adopted for some corrosive liquids in a semiconductor process using the electrically sensing heads with corrosion resistance [3]. However, measuring conductivity is only used for determining the concentration of ionic solutions. Concentration measurements of solutions containing nonionic and weak ionic substances are more reliable when optical measurements are used [4]. The RI measurement of a liquid using a commercial refractometer was performed to further confirm the concentrations through the relationship between RI and concentration [5]. Therefore, some alternative schemes are still attractive based on optical methodology. In surface plasmon resonance (SPR) and total internal reflection (TIR) sensors [6–9], the intensity and phase of the reflected light are changed by the tested liquids covering the sens-

ing surfaces of the transducers. Usually, the contact surface has to be cleaned before the next use. However, oil or organic liquids are not easily removed [2,8]. Therefore, it takes several procedures to reset the clean surface for the next stable measurements. Typically, an SPR sensor is coated with a gold thin film, and the metallic film is easily affected by corrosive solutions. Contact-type SPR sensors are not suitable for such chemical concentration measurements. Therefore, a chemically stable prism made of sapphire is used according to the TIR in the commercial instrument [5].

To overcome these concerns regarding contact, the design of non-contact or non-intrusive measurement has been successfully demonstrated by employing the separations between the tested liquids and the main sensing heads [10–14]. For conductivity measurement the sensing head needs to be in direct contact with the electrons or ions in the liquids in order to transfer the current signal. Therefore, a non-contact technique is difficult to be applied to the conductivity measurement. Thanks to the advantages of remote and non-contact properties in optical sensing technology, it is possible to evaluate a non-contact design by avoiding the inconvenience of a contact-type sensing head. Recently, an image-based interferometry has been successfully demonstrated for the non-intrusive and real time measurements of concentration of fluids [15,16]. According to a geometric optic perspective, the propagation angle change of an incident light is dependent on the relative RI between two mediums based on Snell's Law. The angle difference can induce a lateral displacement change after light passes through the sample container filled with liquids of different RIs. There are rectangular, triangular, and cylindrical shapes for the

\* Corresponding author.

E-mail address: [rctwu@stust.edu.tw](mailto:rctwu@stust.edu.tw) (R.-C. Twu).

designs of liquid containers [10–14]. In a wave optic perspective, an immersion grating in the tested liquids was used to evaluate a diffraction angle or diffraction efficiency change due to the concentration changes [17–19]. A position sensing detector (PSD) is used to measure the position shifts of the beam spots which are induced by the RI difference in the geometric container and the immersion grating [11,13,17]. However the accuracy of displacement measurements is decided by the spot size and resolution of the PSD. To further improve the measurement resolutions, the spatial shift of the probe light after passing through the liquid container can be converted to a phase variation by using a prompt displacement sensor in a heterodyne interferometer [10]. Moreover, the displacement sensors have been demonstrated using SPR and TIR principles [10,20].

To reduce the volume of the optical transducer, a compact module made by combining the individual devices can improve stability and avoid complex alignments. Sometimes, commercially available devices can't fulfill the requirements. Optical birefringent sensors have been successfully demonstrated in the measurements of angular displacement and liquid concentration in our previous works [21–23]. In this article, a compact displacement sensor (CDS) is proposed to be applied to the non-intrusive liquid concentration measurements in the homodyne interferometer. The homemade CDS was fabricated using a cylindrical lens and an attached birefringent plate. By combining with the transparent acrylic flow container, it potentially provides simple and repeatable measurements for salt and hydrochloric acid (HCL) solutions. The proposed non-intrusive measurement is also useful for real-time quality monitoring of a flowing liquid on a production line.

**2. Design of the compact displacement sensor**

Fig. 1 shows the design concept and geometric drawing of the CDS for a lateral displacement measurement. As shown in Fig. 1(a), the birefringent plate of potassium titanyl phosphate (KTP) ( $n_4$ ) is attached to the cylindrical lens ( $n_2$ ) using UV glue ( $n_3$ ). The position **O** is the center of the cylindrical lens. The position **H** represents an incidence point of a probe light on the curved surface of the lens. The distance between positions **O** and **H** is equal to radius ( $r$ ) of the cylindrical lens, which is equal to 10.2 mm. The probe light with two orthogonal polarizations is perpendicular to the base of the cylindrical lens. The distance between positions **O** and **R** is represented by **L**. The incident angle is defined as:

$$\theta_{1i} = \sin^{-1}(L/r). \tag{1}$$

According to Snell's law, the refracted angle in the lens is defined as:

$$\theta_{1r} = \sin^{-1}\left(\frac{n_1}{n_2} \cdot \sin \theta_{1i}\right), \tag{2}$$

where  $n_1$  and  $n_2$  are the refractive indices of air and lens, respectively. The incident angle between the lens and the glue layer is defined as:

$$\theta_{2i} = \theta_{1i} - \theta_{1r} \tag{3}$$

Fig. 1(b) illustrates more detail for the ray traces through the KTP. The refracted angle in the thin glue layer with a thickness of  $t$  is represented by:

$$\theta_{2r} = \sin^{-1}\left(\frac{n_2}{n_3} \cdot \sin \theta_{2i}\right). \tag{4}$$

Since the glue layer is an interlayer between the lens and KTP, the propagation angles of probe light are described in the following equations:

$$n_2 \cdot \sin \theta_{2i} = n_3 \cdot \sin \theta_{2r}, \tag{5a}$$

$$n_3 \cdot \sin \theta_{3i} = n_p \cdot \sin \theta_p, \tag{5b}$$

$$n_2 \cdot \sin \theta_{3i} = n_s \cdot \sin \theta_s. \tag{5c}$$

The incident angle  $\theta_{3i}$  between the glue layer and KTP plate is equal to  $\theta_{2r}$ . Since the thickness of the glue layer and angle change, the  $n_3$  can be replaced by the  $n_2$  in the Eq. (5b) and (5c) according to Eq. (5a). Thus, it means that the parameters ( $n_3$ , and  $t$ ) of the glue layer can be ignored. The different refracted angles of p- and s-waves are represented by  $\theta_p$  and  $\theta_s$  in the birefringent KTP, respectively.  $\theta_p$  and  $\theta_s$  are expressed by:

$$\theta_p = \sin^{-1}\left(\frac{n_2}{n_p} \cdot \sin \theta_{2i}\right), \tag{6a}$$

$$\theta_s = \sin^{-1}\left(\frac{n_2}{n_s} \cdot \sin \theta_{2i}\right). \tag{6b}$$

The KTP is a biaxial birefringent crystal with three different refractive indices named as  $n_x$ ,  $n_y$ , and  $n_z$ . The s-wave is along the z-axis of the KTP crystal, and the p-wave is parallel to the x-y plane. Therefore,  $n_s$  and  $n_p$  are represented by:

$$n_s = n_z, n_p = n_x n_y / \sqrt{n_y^2 \cdot \cos^2 \theta_p + n_x^2 \cdot \sin^2 \theta_p} \tag{7}$$

The phase delay between the p-wave and s-wave emerging from the CDS can be represented by:

$$\begin{aligned} \phi &= \phi_p - \phi_s \\ &= \frac{2\pi}{\lambda} \cdot (n_p \cdot AC - n_s \cdot AB - n_1 \cdot BE) \\ &= \frac{2\pi}{\lambda} \cdot d \cdot \left( \sqrt{n_z^2 - n_2^2 \cdot \sin^2 \theta_{2i}} - \sqrt{n_y^2 - n_2^2 \cdot \frac{n_y^2}{n_x^2} \cdot \sin^2 \theta_{2i}} \right) \end{aligned} \tag{8}$$

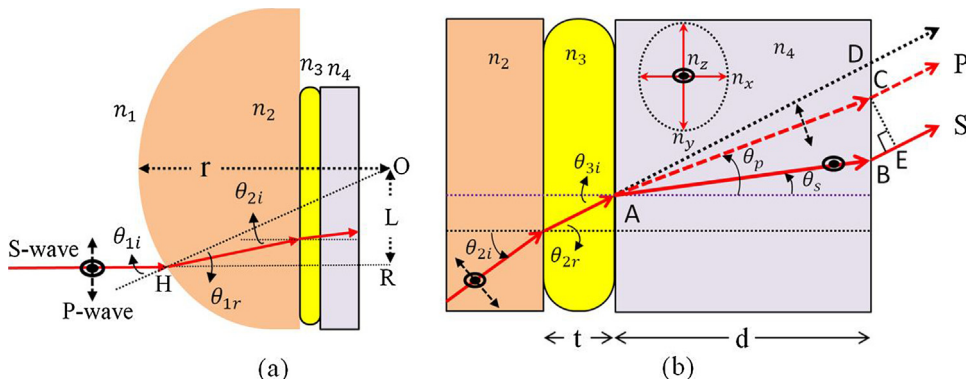


Fig. 1. Geometric drawing of compact displacement sensor: (a) overall layout for the propagation of probe light and (b) the detailed ray paths in the KTP plate.

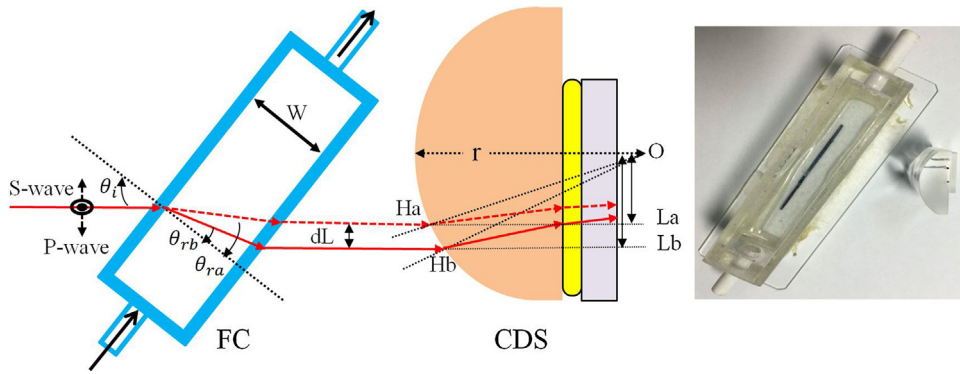


Fig. 2. Schematic diagram and photo of the FC and CDS.

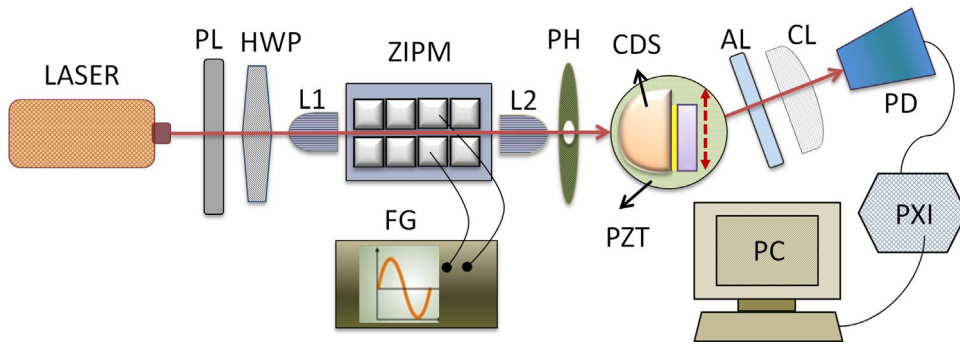


Fig. 3. Schematic of the experimental set-up for the characterization of the CDS.

where  $\lambda$  is the wavelength of the probe light, and  $d$  is the thickness of the KTP plate. According to previous descriptions, the phase delay is a function of  $d$ ,  $n_2$ ,  $n_x$ ,  $n_y$ ,  $n_z$ , and  $\theta_{2i}$ . If the probe light is fixed, the refraction position  $\mathbf{H}$  and lateral distance  $\mathbf{L}$  are changed by the laterally moveable CDS. Thus, it can induce incident angle changes of  $\theta_{2i}$  to change the phase variations. Furthermore, the measured phase variations are adopted to calculate the lateral displacements.

### 3. Non-intrusive concentration measurements

Fig. 2 shows the schematic diagram and photo of the fabricated flow container (FC) and CDS. The flow container is made of 1 mm thick transparent acrylic slides with dimensions of  $40 \text{ mm} \times 10 \text{ mm} \times 10 \text{ mm}$ . The probe light that transmits through the FC with an inner width ( $W=8 \text{ mm}$ ) is perpendicular to the base

of the CDS. The RIs of the injection liquids are increased from  $n_a$  to  $n_b$  as are the concentrations. Usually, the reference liquid ( $n_a$ ) is used as a baseline for comparing the test concentration variations ( $n_b$ ). At an incident angle of  $\theta_i$  of the probe light, the refracted angles  $\theta_{ra}$  and  $\theta_{rb}$ , are described by:

$$\theta_{ra} = \sin^{-1}\left(\frac{1}{n_a} \cdot \sin \theta_i\right), \quad (9a)$$

$$\theta_{rb} = \sin^{-1}\left(\frac{1}{n_b} \cdot \sin \theta_i\right). \quad (9b)$$

As the refracted angle changes from  $\theta_{ra}$  to  $\theta_{rb}$ , the refracted positions shift from  $H_a$  to  $H_b$  on the curved surface of the CDS. The distances of the horizontal lines extension with respect to the cen-

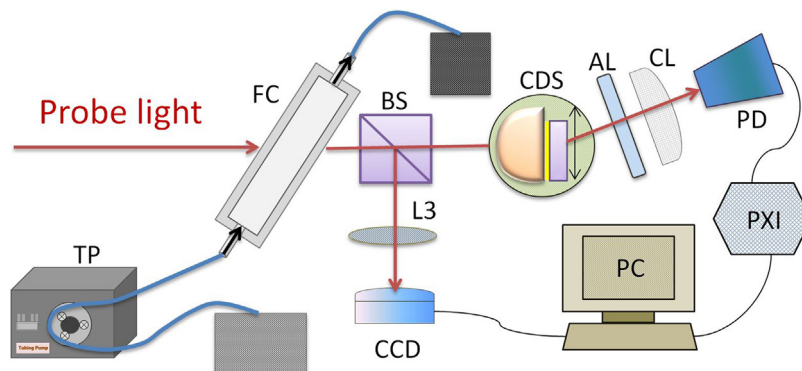


Fig. 4. Setup for non-intrusive concentration measurements of flowing liquid.

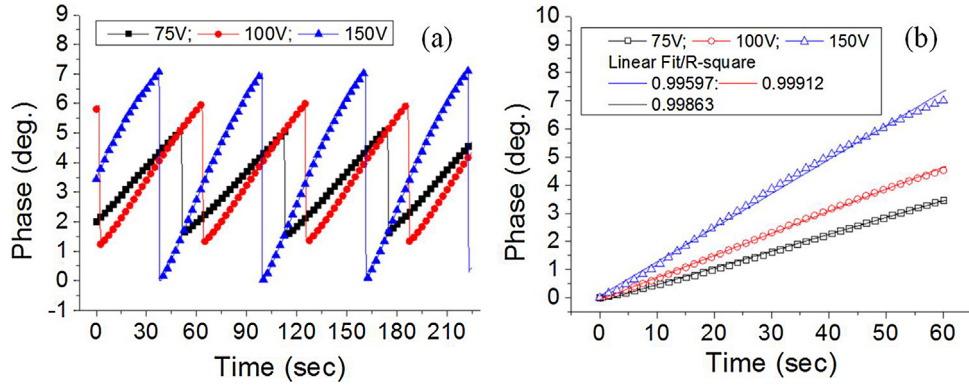


Fig. 5. (a) Phase changes versus time for different applied voltages, (b) Phase variation and linear fit for one period of different voltages.

ter  $\mathbf{O}$  are changed from  $L_a$  and  $L_b$ . The incident angles  $\theta_{1i}$  are decided by the values of  $L_a$  and  $L_b$ . The lateral shift  $dL$  is expressed by:

$$dL = W \cdot \cos\theta_i \cdot (\tan\theta_{ra} - \tan\theta_{rb})$$

$$= W \cdot \sin\theta_i \cdot \cos\theta_i \cdot \left( \frac{1}{\sqrt{n_a^2 - \sin^2\theta_i}} - \frac{1}{\sqrt{n_b^2 - \sin^2\theta_i}} \right) \quad (10)$$

According to the sensing principles of the CDS, the phase variations of the probe light are dependent on the lateral shifts. This means that the measured phase information can be further used to calculate concentration variations through the derived equations.

#### 4. Experimental setup for the CDS and concentration measurement

The experimental setup of the homodyne interferometer used for the characterization of the fabricated CDS is shown in Fig. 3 and includes a linearly polarized light with equal amplitudes for two orthogonal polarizations, which was obtained from a He-Ne laser, a polarizer (PL), and a half-wave plate (HWP). Lenses L1 and L2 were used to focus the input and output beams. A stable homodyne light source with a sinusoidal phase modulation was provided through a lithium niobate waveguide phase modulator (ZIPM) by applying the voltages from a function generator (FG) [22,23]. The homemade ZIPM has advantages of low operation voltage and stable phase modulation for the homodyne and heterodyne interferometers [24,25]. In the homodyne interferometer, the sinusoidal phase modulation and a Fast Fourier transform (FFT) scheme are adopted to improve the phase measurement resolution. A pinhole (PH) was used to block the scattered light. To test the measurement sensitivity of the proposed CDS, the incident positions of the probe light were changed through the movable CDS which was placed on a micro-displacement piezoelectric transducer (PZT) stage. The transmitted light passed through the CDS, an analyzer (AL), and a cylindrical lens (CL) and then, was received by a photodetector (PD). The interferometric signal was connected to a multichannel data acquisition module (PXI), and the phase information is shown on a personal computer (PC). Therein, the phase was interrogated through the FFT technique which was performed in a LabVIEW-based platform [23].

The experimental setup used for the non-intrusive concentration measurements of a flowing liquid is shown in Fig. 4. The probe light from the ZIPM is transmitted through the FC. The liquids with different RIs were injected into the FC by a tubing pump (TP) with a flow rate of 90 sccm (mL/min). The probe light was divided into two different paths by a beam splitter (BS). The transmitted light was used to measure the phase variations in the Homodyne polarization interferometer. At the same time, the reflected light was

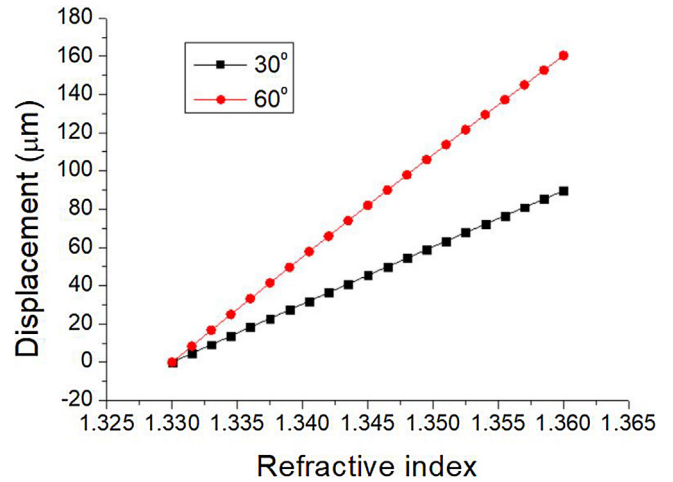


Fig. 6. Lateral displacements versus refractive index of liquid for two different incident angles.

focused through a lens (L3) and then, received by a CCD camera with a pixel resolution of 5.7 μm. The phase variations and the light spot movements were simultaneously measured to compare detection characterizations.

#### 5. Results and discussions

To verify the displacement sensitivity (phase change versus displacement) of the proposed CDS, the incident positions of the probe light were changed by driving the PZT stage with different voltages. The initial position  $\mathbf{H}$  with a vertical distance  $\mathbf{L} = 3.2$  mm was used for the displacement measurements. Fig. 5(a) gives the measurement results of the CDS by applying the different sawtooth voltages. The driving voltages of 75, 100, and 150 V were applied to the driver of the PZT stage, and the corresponding displacements were 20, 26.6, and 40 μm. The measured phase values were 3.55, 4.51, and 7.04 deg for the three voltages. Thus, the values of displacement sensitivity were 0.177, 0.169, and 0.176 (deg/μm) for the different ranges of displacement. The average sensitivity was around 0.174 (deg/μm). Fig. 5(b) gives the linearity between the phase variation and the displacement after linear fits. The values of R-square are 0.9986, 0.9991, and 0.9959 for the displacements of 20, 26.6, and 40 μm, respectively.

According to Eq. (10), the dependence of the lateral displacement on the RI variation can be given in Fig. 6. Assume that RI is 1.33 for the initial baseline liquid and corresponding position; the displacement curves show a good linear tendency in the RIs ranging up to 1.36 for two different incident angles of 30° and 60°. The slope

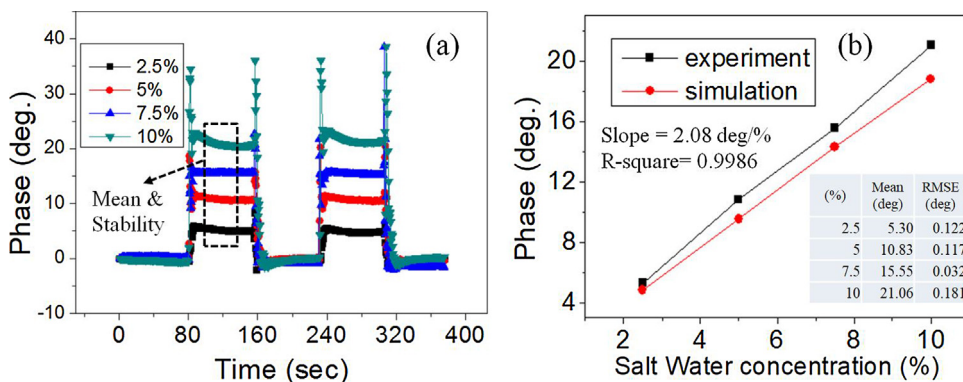


**Fig. 7.** (a) Phase response for the periodic injections between the DI and the different concentrations of SW, (b) Phase variation versus concentration for experimental and simulation results.

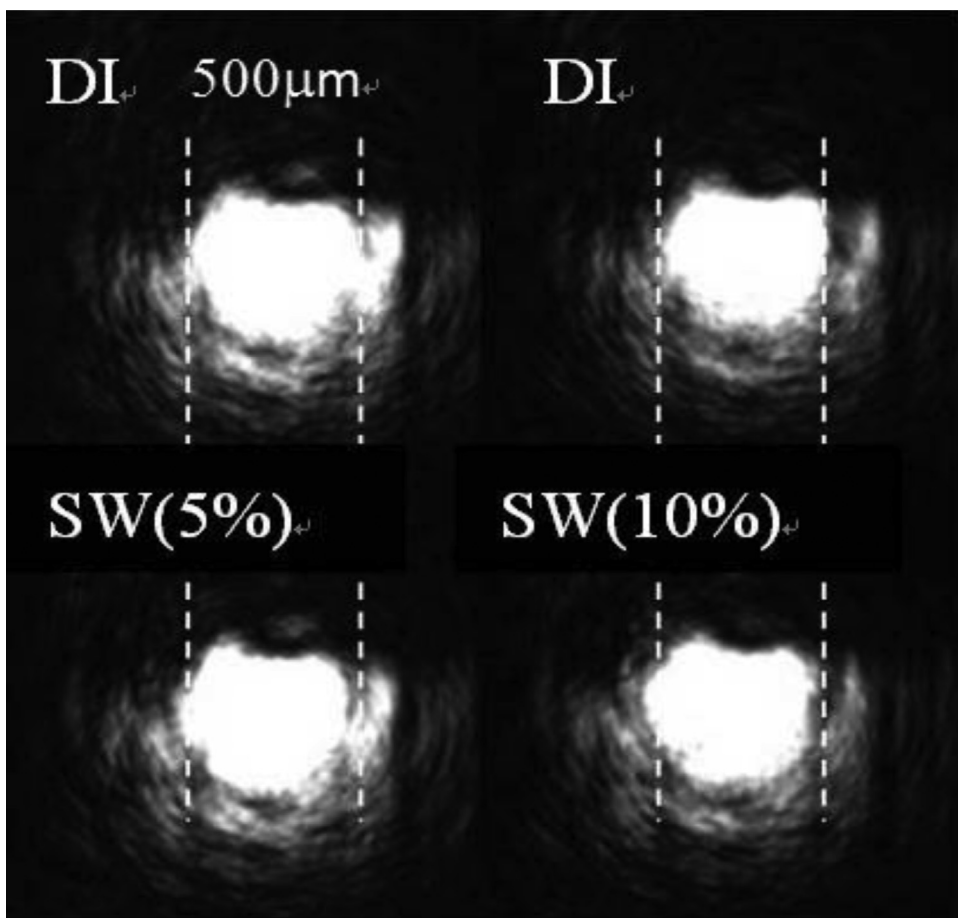


**Fig. 8.** The measurements of spot shifts for different liquids.

of the  $60^\circ$  incident angle is around two times greater than that of the  $30^\circ$  incident angle. Since the lateral displacements are limited for real measurements on the CDS, the adjustable incident angles are flexible for measuring different RIs or concentration ranges.

With the successful verifications between the displacements and phase measurements on the CDS (Fig. 5), and the estimations of the RI induced displacement shifts in the FC (Fig. 6), it shall be possible to combine them for non-intrusive measurements. In the experiments, the initial incident angle  $\theta_i$  and distance  $L_a$  are  $60^\circ$  and 3.2 mm, respectively. The positions of transmitted lights on the CDS were shifted through the FC by injecting different liquids of deionized water (DI) and salt water (SW) with each period of

80 s. Fig. 7(a) illustrates the phase response for periodic exchanges between DI and different concentrations of SW. The weight percentages of the SW were 2.5%, 5%, 7.5%, and 10%. The corresponding RIs, 1.338, 1.343, 1.384, and 1.353, were used for the simulations [26]. The response time for the stable phase measurements during the liquids exchanged is mainly dependent on the design of flow container and the flowing speed. According to the experimental results, the rising and falling times between the DI and SW liquids are of around 4.5 and 6 s, respectively. To represent the relationship between the measured phase and the concentration, as shown in Fig. 7(b), the mean phase and stability values of each concentration were taken by considering a measured phase of 40 s in the first

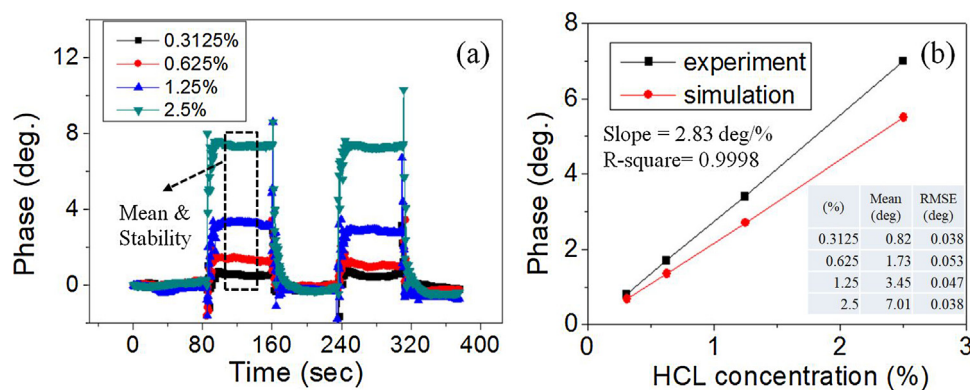


**Fig. 9.** (a) Phase response for periodic injections between the DI and the different concentrations of HCL, (b) Phase variation vs. concentration for experimental and simulation results.

middle period, as shown in Fig. 7(a). To clearly discuss the measurement stability based on a proper error analysis, a root mean square error (RMSE) of the measured data is used to express the phase stability in the measurements. The summarized table of the mean values and RMSEs is shown in the inset of Fig. 7(b). Comparisons between the experimental results and the simulations are shown in Fig. 7(b). Both of the phase curves show good linearity between the phase and concentration variations. The concentration sensitivity is defined as a slope of phase variation versus concentration. The slope of the experimental phase results after the linear fit is 2.08 (deg/%). The corresponding R-square is 0.9986. Based on the best phase stability 0.032 deg during flowing SW, a resolution of 0.015% on the non-intrusive measurements of SW concentration is achievable.

To compare the measurement capability between the CCD and phase measurements, the spots shifted horizontally during the switch between the DI and the different SW solutions (5% and 10%) are shown in Fig. 8. The probe beam diameter is around 500  $\mu\text{m}$ . The position shifts were small even in the liquids that changed from the DI to SW (10%). This means that the phase measurement is more sensitive to analyze concentration variations.

Fig. 9(a) illustrates the phase response for periodic exchanges between the DI and different weight percentages of hydrochloric acid (HCL) solutions. The rising and falling times between the DI and HCL liquids are of around 5.5 and 6.5 s, respectively. The concentrations were 0.3125%, 0.625%, 1.25%, and 2.5%. The corresponding RIs, 1.3337, 1.3344, 1.3358, and 1.3387, were used for the simulations [5]. Comparisons between the experimental results and the simulations are shown in Fig. 9(b). Both of the phase curves show good linearity between the phase and concentration variations. The slope and R-square of the experimental phase results after a linear fit were 2.83 (deg/%) and 0.9998, respectively. The summarized table of the mean values and RMSEs is shown in the inset of Fig. 9(b). Based on the best phase stability 0.038 deg during flowing HCL, a resolution of 0.013% on the measurements of HCL concentration is achievable.

## 6. Conclusions

The proposed CDS has been successfully demonstrated for non-intrusive measurements on concentration variations of flowing liquids. The measurement resolutions were 0.015% and 0.013% for the SW and HCL solutions, respectively. In comparison to the contact-type designs, the sample container separated with a sensing head can reduce cleaning steps and avoid damage to the sensing head. Monitoring of concentration variations is especially essential in some erosive or dangerous chemicals during manufacturing. The properties of viscosity or causticity need reliable measurements for

cleaning sensing heads. A disposable and cheap acrylic container will provide simple and repeatable measurements for some special solutions such as oil-related products and organic chemicals. Moreover, the measured RIs in dynamic ranges are easily adjusted by tuning the incident angles at the flow container.

## Acknowledgement

This study was supported in part by the Ministry of Science and Technology in Taiwan under grant number MOST 105-2221-E-218-014.

## References

- [1] B. Schreiber, C. Wacinski, R. Chiarello, Index of refraction as a quality control metric for liquids in pharmaceutical manufacturing, *Pharm. Eng.* 33 (2013) 1–7.
- [2] Y.J. Cho, T.E. Kim, B. Gil, Correlation between refractive index of vegetable oils measured with surface plasmon resonance and acid values determined with the AOCS official method, *LWT-Food Sci. Technol.* 53 (2013) 517–521.
- [3] Rosemount Analytical Inc., <http://www.RosemountAnalytical.com>.
- [4] M.W. Johnson, K. Golden, G. Gilleskie, J. Pancorbo, R.R. Vilhena, Comparison of concentration measurement technologies in bioprocess solutions, *Bioprocess Int.* 13 (2015) 60–67.
- [5] Electron Machine Corporation, <http://www.electronmachine.com>.
- [6] M. McClimans, C. LaPlante, D.B.S. Bali, Real-time differential refractometry without interferometry at a sensitivity level of  $10^{-6}$ , *Appl. Opt.* 45 (2006) 6477–6486.
- [7] M. Maisonneuve, I.-H. Song, S. Patskovsky, M. Meunier, Polarimetric total internal reflection biosensing, *Opt. Express* 19 (2011) 7410–7416.
- [8] M. Milanese, A. Ricciardi, M.G. Manera, A. Colombelli, G. Montagna, A. de Risi, R. Rella, Real time oil control by surface plasmon resonance transduction methodology, *Sens. Actuators A Phys.* 223 (2015) 97–104.
- [9] W.C. Lawa, P. Markowicz, K.T. Yong, I. Roy, A. Baev, S. Patskovsky, A.V. Kabashin, H.P. Ho, P.N. Prasad, Wide dynamic range phase-sensitive surface plasmon resonance biosensor based on measuring the modulation harmonics, *Biosens. Bioelectron.* 23 (2007) 627–632.
- [10] K.H. Chen, J.H. Chen, S.W. Kuo, T.T. Kuo, M.H. Lai, Non-contact method for measuring solution concentration using surface plasmon resonance apparatus and heterodyne interferometry, *Opt. Commun.* 283 (2010) 2182–2185.
- [11] V. Krishna, C.H. Fan, J.P. Longtin, Real-time precision concentration measurement for flowing liquid solutions, *Rev. Sci. Instrum.* 71 (2000) 3864.
- [12] H.K. Singh, N. Chamuah, D. Sarkar, T. Bezboruah, Non-intrusive technique for measuring refractive index of clear and transparent liquids, *IEEE Sens.* 14 (2014) 313–314.
- [13] S. Nemoto, Measurement of the refractive index of liquid using laser beam displacement, *Appl. Opt.* 31 (1992) 6690–6694.
- [14] O. Vilitis, P. Shipkovs, D. Merkulov, Determining the refractive index of liquids using a cylindrical cuvette, *Meas. Sci. Technol.* 20 (2009) 117001.
- [15] S.S. Varma, S. Srinivas Rao, Atul Srivastava, Simultaneous measurement of thermal and solutal diffusivities of salt-water solutions from a single shot dual wavelength interferometric image, *Exp. Therm. Fluid Sci.* 81 (2017) 123–135.
- [16] S.S. Varma, Atul Srivastava, Real time two color interferometric technique for simultaneous measurements of temperature and solutal fields, *Int. J. Heat Mass Transfer* 98 (2016) 662–674.
- [17] V.M. Durán-Ramírez, A. Martínez-Ríos, J.A. Guerrero-Viramontes, J. Muñoz-Maciel, F.G. Peña-Lecona, R. Selvas-Aguilar, G. Anzueto-Sánchez, Measurement of the refractive index by using a rectangular cell with a fs-laser engraved diffraction grating inner wall, *Opt. Express* 22 (2014) 29899–29906.

- [18] L.F.G. Dib, E.A. Barbosa, Immersed diffraction grating refractometers of liquids, *Appl. Opt.* 55 (2016) 8582–8588.
- [19] Sergio Calixto, Neil C. Bruce, Martha Rosete-Aguilar, Diffraction grating-based sensing optofluidic device for measuring the refractive index of liquids, *Opt. Express* 24 (2016) 180–190.
- [20] K.H. Chen, H.S. Chiu, J.H. Chen, Y.C. Chen, An alternative method for measuring small displacements with differential phase difference of dual-prism and heterodyne interferometry, *Measurement* 45 (2012) 1510–1514.
- [21] R.C. Twu, C.S. Wang, Birefringent-refraction transducer for measuring angular displacement based on heterodyne interferometry, *Appl. Sci.* 6 (2016) 208.
- [22] R.C. Twu, G.M. Chen, J.Y. Chen, N.Y. Yan, A fluidic birefringent sensor for concentration measurements of chemical solutions in homodyne interferometer, *Appl. Sci.* 6 (2016) 318.
- [23] R.C. Twu, C.W. Hsueh, Phase interrogation birefringent-refraction sensor for refractive index variation measurements, *Sens. Actuators A Phys.* 253 (2017) 85–90.
- [24] R.C. Twu, Y.H. Lee, H.Y. Hou, A comparison between two heterodyne light sources using different electro-optic modulators for optical temperature measurements at visible wavelengths, *Sensors* 10 (2010) 9609–9619.
- [25] R.C. Twu, K.W. Wang, H.Y. Tu, Scanning phase-interrogation polarimetry for wide dynamic optical activity measurement, *Sens. Actuators B Chem.* 249 (2017) 725–730.
- [26] Yunus W. Mahmood bin Mat, Rahman Azizan bin Abdul, Refractive index of solutions at high concentrations, *Appl. Opt.* 27 (1988) 3341–3343.

## Biographies

**Ruey-Ching Twu** received the Ph.D. degree in Graduate Institute of Electro-Optical Engineering (2000) from National Taiwan University, Taiwan. He is currently a professor at Southern Taiwan University of Science and Technology, Department of Electro-Optical Engineering. His research interests include integrated optics, optical metrology systems, and sensors.

**Jheng-Yu Chen** received his M.Sc. degree in Department of Electro-Optical Engineering (2016) from Southern Taiwan University of Science and Technology, Taiwan. His research interests include optical transducer designs, and optical sensing applications.